Oral administration of L-mR18L, a single domain cationic amphipathic helical peptide, inhibits lesion formation in ApoE null mice[S]

Shaila P. Handattu,* Geeta Datta,* Richard M. Epand,[§] Raquel F. Epand,[§]
Mayakonda N. Palgunachari,* Vinod K. Mishra,* Candyce E. Monroe,* Tamara D. Keenum,*
Manjula Chaddha,* G. M. Anantharamaiah,*[,†] and David W. Garber[1][,]*

Atherosclerosis Research Unit, Departments of Medicine* and Biochemistry and Molecular Genetics,[†]
University of Alabama, Birmingham, AL; and Department of Biochemistry and Biomedical Sciences,[§]
McMaster University, Hamilton, Ontario, Canada

Abstract We have shown that Ac-hE18A-NH$_2$, a dual-domain cationic apolipoprotein-mimetic peptide, reduces plasma cholesterol levels in dyslipidemic mice. Two single-domain cationic peptides based on the lytic class L peptide 18L were developed to test the hypothesis that a single-domain cationic amphipathic peptide can reduce atherosclerosis in apolipoprotein (apo)E null mice when orally administered. To incorporate anti-inflammatory properties, aromatic residues were clustered in the nonpolar face similar to peptide 4F, resulting in modified 18L (m18L). To reduce lytic properties, the Lys residues of 18L were replaced with Arg with the resulting peptide called modified R18L (mR18L). Biophysical studies showed that mR18L had stronger interactions with lipids than did m18L. Peptide mR18L was also more effective than m18L in promoting LDL uptake by HepG2 cells. ApoE null mice received normal chow or chow containing m18L or mR18L for six weeks. A significant reduction in plasma cholesterol and aortic sinus lesion area was seen only in the mR18L group. Plasma from mice administered mR18L, unlike those from the control and m18L groups, did not enhance monocyte adhesion to endothelial cells. Thus oral administration of mR18L reduces plasma cholesterol and lesion formation and inhibits monocyte adhesion.—Handattu, S. P., G. Datta, R. M. Epand, R. F. Epand, M. N. Palgunachari, V. K. Mishra, C. E. Monroe, T. D. Keenum, M. Chaddha, G. M. Anantharamaiah, and D. W. Garber. **Oral administration of L-mR18L, a single domain cationic amphipathic helical peptide, inhibits lesion formation in ApoE null mice.** *J. Lipid Res.* 2010. **51:** 3491–3499.

Supplementary key words   atherosclerosis • metabolism • animals • lipids • cholesterol

As apolipoprotein (apo)A-I possesses tandem repeating class A amphipathic helical motifs, several investigators (including our own laboratory) have developed peptides that possess the class A amphipathic helical motif and have shown that, similar to apoA-I, several of these peptides not only interact with phospholipids to form nascent HDL-like peptide-lipid discoidal complexes but also possess both anti-inflammatory and cellular cholesterol effluxing properties (1–3). Several papers have been published using 4F and D-4F peptides to demonstrate that the peptides inhibit or slow down the onset of several inflammatory diseases, including atherosclerosis (reviewed in Ref. 4). When 4F is synthesized from all D amino acids, the resulting D-4F is orally active and can be administered either in drinking water or mixed with food to inhibit inflammatory processes (5). However, not all of the class A peptides are anti-inflammatory (6, 7). It has been shown that the clustering of aromatic residues on the nonpolar face of a class A amphipathic helical motif favors its association with oxidized phospholipid (6–9).

An ideal strategy for inhibiting atherosclerosis would not only decrease plasma cholesterol levels but also increase anti-inflammatory properties. ApoE, the protein

Abbreviations: Apo, apolipoprotein; BAEC, bovine aortic endothelial cell; CLiP, column lipoprotein profile; DSC, differential scanning calorimetry; FPLC, fast-performance liquid chromatography; HSPG, heparan sulfate proteoglycan; MLV, multilamellar vesicle; POPC, palmitoyloleoyl phosphatidylcholine; SOPC, stearoyloleoyl phosphatidylcholine.
[1] To whom correspondence should be addressed.
   e-mail: dgarber@uab.edu
[S] The online version of this article (available at http://www.jlr.org) contains supplementary data in the form of one table and three figures.

component of VLDL and HDL, has been shown to have anti-atherogenic properties (10, 11). Mice overexpressing apoE have accelerated clearance of plasma lipoproteins (10). Injection of apoE into cholesterol-fed rabbits reduces atherogenic plasma lipoproteins (11), and deletion of the apoE gene in mice produces spontaneous atherosclerosis (12). ApoE also exerts vascular protective effects. On the basis of the idea that apoE possesses the putative receptor binding domain (141–155 region of apoE) at the N-terminus and a lipid binding domain at the C terminus, we designed a dual-domain peptide Ac-hE18A-NH$_2$ in which residues 141–150 of apoE, LRKLRKRLLR, is covalently bound to the model class A peptide 18A (2). This peptide is capable of reducing plasma cholesterol via hepatic uptake and has anti-inflammatory properties (13–15). However, this peptide has only been shown to be active when intravenously administered.

In search for an orally active peptide possessing both cholesterol reducing and anti-inflammatory properties, we turned our attention to the cationic model class L (lytic) peptide studied by us previously (16). Class A peptides were able to inhibit 18L-induced lysis of erythrocytes (16). We also observed that modification of the Lys residues by dimethylation or replacement by Arg reduced the lytic properties of 18L by disrupting the inverted wedge-shape (16). Our previous observations suggest that the presence of a cluster of aromatic amino acids increase π-electron clustering at the center of the nonpolar face of the class A peptide and promote a selective association of the peptide to oxidized lipids, imparting anti-inflammatory properties to the peptides (6, 17). Therefore, we modified the 18L peptide sequence (**Fig. 1A**) by incorporating aromatic amino acids at the center of the nonpolar face (Fig. 1B), generating modified 18L (m18L). We have shown that the ability of class L analogs to lyse membranes and induce inverted lipid phase was reduced by decreasing the bulk of an interfacial residue, increasing the angle subtended by the polar face, or increasing the bulk of basic residues (16). Thus, m18L was further modified by substituting Lys residues with Arg to yield mR18L with the sequence Ac-GFRRFLGSWARIYRAFVG-NH$_2$ (Fig. 1C). In this study, we present evidence demonstrating that while mR18L, with

Arg (R) as the basic amino acid, was able to enhance uptake of atherogenic lipoproteins by hepatocytes, the corresponding Lys analog (m18L) was less active. In addition, oral administration of mR18L, but not m18L, inhibited atherosclerotic lesion formation in apoE null mice. Furthermore, the plasma from mR18L-administered mice did not enhance monocyte adhesion to bovine aortic endothelial cells (BAEC), whereas the plasma from control (chow-fed) and m18L-administered mice did not prevent monocyte recruitment by BAEC.

MATERIALS AND METHODS

Materials

Peptide m18L with the sequence Ac-G-F-K-K-F-L-G-S-W-A-K-I-Y-K-A-F-V-G-NH$_2$ and its Arg analog (mR18L; all of the Lys in m18L replaced by Arg) were synthesized by the solid phase peptide synthesis method using fluorenylmethyloxycarbonyl (FMOC) amino acids and suitable protected amino acids as described previously (13). The peptides were purified by preparative HPLC, and the purity and identity of the peptides were determined by analytical HPLC and mass spectra. ^{14}C-labeled peptides were synthesized by blocking the N-terminus with ^{14}C-acetic acid. The rest of the procedures for the cleavage of the peptide from the resin and purification and identification of the required peptide were done according the procedure described previously (6).

ApoE null female mice were purchased from the Jackson laboratory (Bar Harbor, ME) and were maintained on a chow diet (Ralston Purina). Peptide concentrations were determined as described previously (6, 7). Lipids were purchased from Avanti Polar Lipids (Birmingham, AL). All protocols involving mice were approved by the University of Alabama at Birmingham Institutional Animal Care and Use Committee.

Right-angle light scattering measurements

Association of these peptides with palmitoyloleoyl phosphatidylcholine (POPC) was determined by following the dissolution of POPC multilamellar vesicles (MLV) by right-angle light scattering using an SLM 8000C photon counting spectrofluorometer as described (18). POPC MLV were prepared by evaporating a chloroform:methanol (2:1) solution of POPC (Avanti Polar Lipids) under nitrogen and hydrating the lipid film with phosphate buffered saline (pH 7.4). The sample, containing 100 μM of POPC and an equimolar amount of peptide, was maintained at
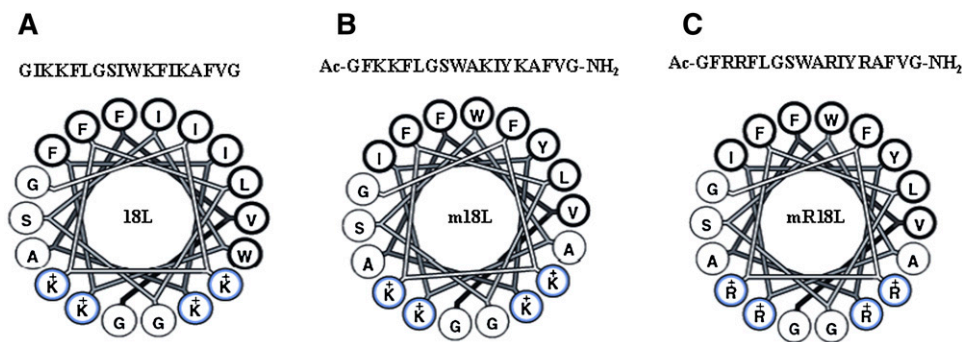

Fig. 1. Helical wheel diagrams of the model class L synthetic peptide analog 18L (A), the Lys analog m18L (B), and the Arg analog mR18L (C). Bold circles represent hydrophobic amino acid residues. Aromatic residues are at the center of the hydrophobic face in m18L and mR18L while, with the exception of the K to R substitution, the hydrophilic face is the same in all three peptides.

25°C and continuously stirred. Turbidity clarification was monitored at 400 nm for 30 min.

Differential scanning calorimetry

Stearoyloleoyl phosphatidylcholine (SOPC) with or without cholesterol were codissolved in chloroform:methanol (2:1, v/v). For samples containing peptide, an aliquot of a solution of the peptide in methanol was added to the lipid solution in chloroform:methanol. The solvent was then evaporated under a stream of nitrogen with constant rotation of the test tube to deposit a uniform film over the bottom third of the tube. Last traces of the solvent were removed by placing the tube under high vacuum for at least 3 h. The lipid film was then hydrated with 20 mM PIPES, 1 mM EDTA, 150 mM NaCl with 0.002% NaN_3, pH 7.4 and suspended by intermittent vortexing and heating to 50°C over a period of 2 min under argon.

Measurements were made using a Nano Differential Scanning Calorimeter (Calorimetry Sciences Corporation, Lindon, UT). Each sample was scanned with two or three cycles of heating and cooling between 0 and 100°C. The scan rate was 2°C/min with a delay of 5 min between sequential scans in a series to allow for thermal equilibration. The features of the design of this instrument have been described (19). Differential scanning calorimetry (DSC) curves were analyzed by using the fitting program DA-2, provided by Microcal Inc. (Northampton, MA) and plotted with Origin version 7.0.

Cellular uptake by HepG2 cells

The uptake of LDL by HepG2 cells was measured as described by Goldstein and Brown (20) and detailed in Ref. 13. HepG2 cells were grown in DMEM containing 10% fetal calf serum (FCS) and penicillin-streptomycin-amphotericin in 6-well plates and used after reaching 75–90% confluency (two or three days). The seeding density of cells used was 1.5×10^5 to 3×10^5 cells/ml of medium. Cells were incubated with medium containing lipoprotein-deficient serum (LPDS) for 24 h prior to use. The peptide was allowed to associate with LDL by incubating ^{125}I-LDL for 1 h at 4°C. The peptides were found to bind LDL similarly (supplementary Table I). Cells were incubated with peptide-treated ^{125}I-LDL (or control LDL) at 4°C for 2 h. After washing four times with ice-cold PBS containing 2 mg/ml BSA to remove nonspecifically bound lipoprotein, specifically bound LDL was released by washing with heparin. Similar amounts of label were removed by heparin washing (m18L, 43.2%; mR18L, 45.6% of total cpm added to the wells). The cells were then dissolved in 0.1N NaOH and counted. The counts reflected the amount of LDL that was internalized.

Intravenous administration of the peptides and acute effect on plasma cholesterol in apoE null mice

To determine if the peptides possess short-term effects on decreasing plasma cholesterol, 75 μg of the peptides in 100 μl saline was administered intravenously (n = 4 in each group) to apoE null female mice. A control group of three apoE null mice received vehicle (saline). Blood was drawn retro-orbitally at 0 min, 2 min, and 5 h. Plasma cholesterol levels were determined using a commercially available kit (Infinity cholesterol reagent, Thermo Scientific). The effect of proteoglycans on peptide-mediated cholesterol reduction was assessed by injecting saline or heparinase (50 units/mouse; Sigma) intravenously 5 min before peptide injection.

Bioavailability of ^{14}C-labeled peptides in plasma upon oral administration by gavage

^{14}C-labeled m18L and mR18L in saline were administered by gavage to fasting female apoE null mice. The gavage volume for m18L was 150 μl at a concentration of 0.75 mg/ml and contained 1.38×10^6 cpm. The gavage volume for mR18L was 150 μl at a concentration of 0.67 mg/ml and contained 4.85×10^5 cpm. Mice were bled at various time points, and ^{14}C radioactivity was measured in each of the samples. Three samples were taken at each time point from different mice. As the specific activity of m18L was higher than that for mR18L, plasma levels were expressed as % gavaged cpm. Plasma taken 15 min postgavage was analyzed by reverse-phase HPLC for content of intact ^{14}C-labeled peptide and ^{14}C acetate.

Oral administration of peptides and effect on plasma cholesterol and lesion

To determine if oral administration of peptide lowers plasma cholesterol and reduces aortic lesions, four-week old apoE null female mice were administered chow-containing peptide (1 mg peptide/4 g of chow) for six weeks. Peptide was premixed with powdered normal mouse chow (powdered rodent diet #2018-M, Harlan-Teklad), which was then moistened, pelleted, and dried. Control chow was prepared the same way but omitted the peptide. Plasma was collected by retro-orbital bleeding at baseline, three weeks, and six weeks. At the end of six weeks, hearts were excised and stored in 0.9% saline for about 1 h to permit heart muscle to relax. They were then fixed in phosphate buffered 4% formaldehyde until sectioned. Histological evaluations were performed as described earlier (21). Briefly, hearts were fixed for at least 1 week in the phosphate-buffered formaldehyde solution. After the lower two-thirds of the hearts were removed, the remaining tissue was frozen in freezing medium (OCT Tissue-Tek; Miles Laboratories, Elkhart, IN) and sectioned in a cryostat at −20°C. Alternate 20 μm sections were saved on slides and observed for the beginning of the aortic root. Sections were then collected for an additional 600 μm, or until the aortic cross-section was rounded, and the valve cusps were no longer evident. Slides were stained with Oil Red O and counterstained with hematoxylin. Stained lesion cross-sectional areas were measured in consecutive slides 80 μm apart by image analysis (SigmaScan Pro; SPSS Science, Chicago, IL), and the average lesion area was determined over the 400 μm length sliding window (five slides, with each five-slide window beginning with the next consecutive slide). The five-slide window that provided the greatest mean lesion area was used for analysis.

Plasma cholesterol profiles were analyzed using the column lipoprotein profile CLiP method, which employs fast-performance liquid chromatography (FPLC) followed by a postcolumn reactor where cholesterol reagent is mixed with the column eluent (22).

Monocyte adhesion assays

The ability of plasma from peptide-treated and control animals to promote monocyte adhesion to endothelial cells was assessed by bovine aortic endothelial cell (BAEC) assay (7, 23). BAEC were grown to 80% confluency in 24-well plates. They were treated with medium alone, lipopolysaccharide (1μg/ml, as a positive control), or 200 μl of plasma from control or peptide-treated (m18L or mR18L) mice (each tested sample was pooled from 2–3 mice) and incubated for 6 h. They were then washed with PBS and incubated with calcein-labeled THP-1 monocytes for 1 h at 37°C. [THP-1 monocytes were labeled with calcein as per the manufacturer's instructions (Invitrogen Molecular Probes, Carlsbad, CA)]. The BAEC were washed, and fluorescence was measured using an excitation wavelength of 495 nm and an emission at 517 nm.

Statistical analysis

Groups were compared by one way ANOVA, and posthoc two-tailed Student's *t*-tests were performed on groups found to be

significantly different by ANOVA. Groups were considered to be significantly different when $P < 0.05$.

RESULTS

Cationic single-domain peptides m18L and mR18L associate with phospholipids

Association of peptides with multilamellar POPC vesicles converts turbid suspensions into clear solutions due to peptide:lipid complex formation (1, 2). This can be measured by right-angle light scattering. As shown in **Fig. 2**, addition of both m18L and mR18L peptide solution to MLV of POPC clarifies POPC MLV to form complexes. However, mR18L (75% clarification) appears to clarify POPC to a greater extent than m18L (60% clarification). These results indicate that the peptides are capable of associating with lipoproteins. In a mixing experiment, [^{14}C]m18L or [^{14}C]mR18L was added to apoE null plasma and subjected to ultracentrifugation at a density of 1.21. Of the total radioactivity, 46.97% of m18L and 46.04% of mR18L (mean of two observations) were in the lipoprotein fractions. Although attempts were made to optimize the mobile phase, analyses by FPLC could not be conducted as the peptides strongly adsorbed to the column matrix.

Stronger interactions of mR18L than m18L with phospholipids

DSC can be used to measure the gel-to-liquid crystalline phase transition of phospholipids. For a single molecular component phospholipid, this transition is highly cooperative and gives rise to a sharp endothermic peak in the DSC thermogram. POPC has palmitoyl and SOPC has stearoyl fatty acyl chain in the sn-1 position. The sn-2 chain is identical in both POPC and SOPC. Thus, the lipid SOPC used for these experiments was based on the relative ease of observing phase transition using DSC, and unlike POPC, its phase transition temperature is above 0°C (**Fig. 3**). The phase transition of this lipid is not greatly affected by the presence of 7.5 mol% m18L, but the transition is broadened and markedly reduced in enthalpy with 5 mol% of

Fig. 2. Both m18L and mR18L clarify POPC suspensions. Shown are representative POPC clarification curves of the relative right-angle light scattering of the dissolution of POPC MLV by single-domain peptides as a function of time. An equimolar concentration of peptide and POPC (100 μM) was monitored at 400 nm. POPC (●), m18L (○), and mR18L (▼). MLV, multilamellar vesicle; POPC, palmitoyloleoyl phosphatidylcholine.

the peptide mR18L (Fig. 3). Higher mole fractions of mR18L cause an even greater reduction in the transition enthalpy (data not shown). These results indicate that the insertion of the mR18L peptide into bilayers of the zwitterionic lipid SOPC is much greater than that of m18L.

mR18L is more effective in segregating cholesterol than is m18L

Cholesterol is known to markedly broaden and reduce the phase transition enthalpy of phosphatidylcholines. We have used this phenomenon to assess the extent of segregation of cholesterol and phospholipids (24). Peptide-induced separation of cholesterol and phosphatidylcholine can result from the peptide preferentially interacting with one of the two lipid components. Preferential interaction with cholesterol-rich domains leads to separation of a cholesterol-depleted domain of phospholipid that gives rise to a larger and sharper gel-to-liquid crystalline transition. However, preferential interaction with phosphatidylcholine results in less change in this transition. Both mechanisms of phase separation have been observed to give rise to cholesterol crystallites, presumably arising from cholesterol-rich domains in which the cholesterol has passed its solubility limit in the membrane. This later type behavior has been observed with the peptide 4F (25). Using a mixture of 60% SOPC and 40% cholesterol, no peaks corresponding to cholesterol crystallites were observed (**Fig. 4**). There is a small and broad peak that could be seen more clearly in cooling scans, corresponding to the liquid crystalline-to-gel transition at about 7°C. Addition of only 5 mol% mR18L resulted in the appearance of distinct peaks corresponding to the polymorphic transition of anhydrous cholesterol with its characteristic hysteresis, appearing shifted about 15 degrees to lower temperature on cooling compared with heating (Fig. 4). In contrast, these cholesterol crystallite transitions were not observed when the peptide m18L was substituted for mR18L. We also made samples at other ratios of SOPC:cholesterol and other mol fractions of added peptide between 5 and 15%. At an SOPC:cholesterol ratio of 7:3, no cholesterol crystallite transitions were observed for any of the samples (data not shown). At the 6:4 ratio of SOPC:cholesterol, no cholesterol crystallites were observed up to 15 mol% m18L. For mR18L, the amount of cholesterol crystallites actually decreased with increased peptide concentration, suggesting that the peptide was beginning to bind to cholesterol-rich domains at higher peptide concentration. Finally for a 1:1 mixture of SOPC:cholesterol, cholesterol crystallites were detected at 5, 10, and 15 mol% mR18L, but for m18L, cholesterol crystallite peaks were observed only in the first heating scan and not in subsequent scans (data not shown).

Fluorescence titrations were done with m18L and mR18L and oxidized lipids. The results in terms of binding affinity are summarized in **Table 1**, together with values from our earlier study on 2F and 4F (9). Peptide m18L behaves very similarly to 2F, while peptide mR18L binds oxidized lipids better than m18L. However, it is not as potent in binding oxidized lipids as is 4F. Thus, not all peptides with aromatic lipid clusters have potent anti-atherogenic
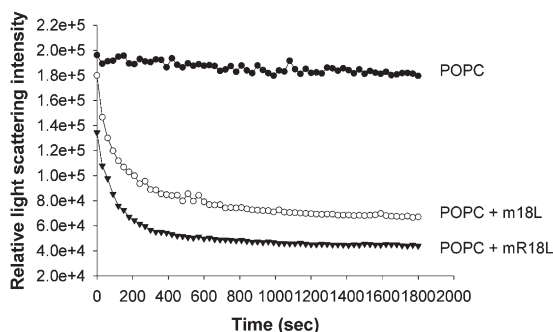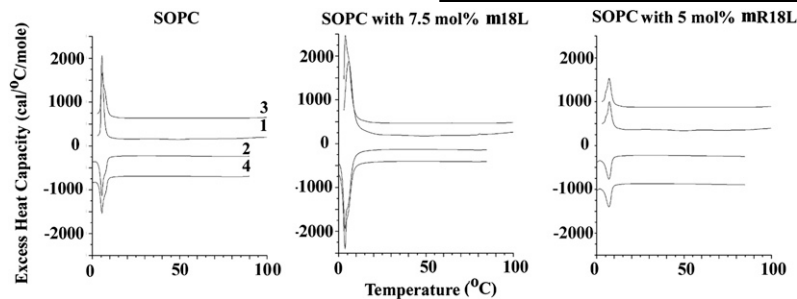
Fig. 3. Differential scanning calorimetry of SOPC alone and with 7.5 mol% m18L or with 5 mol% mR18L. Scan rate 2K/min. Lipid concentration 2.5 mg/ml in 20 mM PIPES, 1 mM EDTA, and 150 mM NaCl with 0.002% NaN_3, pH 7.4. Sequential heating and cooling scans were done between 0 and 100°C. Numbers are the order in which the scans were carried out, with scans 1 and 3 being heating scans, each of which was followed by cooling scan 2 or 4. Scans are displaced along the Y axis for clarity of presentation. SOPC, stearoyloleoyl phosphatidylcholine.

activity; therefore, the nature of the hydrophilic face is also important.

Peptide mR18L enhances the uptake of LDL by HepG2 cells to a greater extent than m18L

The effect of the single-domain cationic peptides on the uptake of ^{125}I-LDL by HepG2 cells was examined. LDL uptake was significantly enhanced by m18L and mR18L (10 μg/ml) to different extents (**Fig. 5**). The substitution of Lys residues of m18L with Arg residues in mR18L appears to further enhance the ability of these peptides to mediate LDL uptake (Fig. 5). Thus, it may be that the cluster of positively charged residues in Arg facilitates a greater interaction with heparan sulfate proteoglycan (HSPG) on the surface of hepatocytes. Here we show that mR18L enhanced LDL uptake almost 10 times more than vehicle treatment and was twice as effective as m18L-induced LDL uptake (which was 5 times greater than controls).

Effect of intravenous administration of peptides on plasma cholesterol

The cholesterol-lowering abilities of peptides mR18L and m18L were determined in apoE null mice. A single dose of peptide (75 μg) administered intravenously showed that both m18L and mR18L were capable of reducing the plasma cholesterol level at 5 min to the same extent (**Fig. 6A**). At the 5 h time point, the peptide mR18L showed significantly lower levels of plasma cholesterol compared with m18L and saline-administered mice. Preinjection of heparinase before peptide administration partially blocked peptide-mediated cholesterol reduction (Fig. 6B). The failure to fully block the effects of peptides on cholesterol levels may have been due to insufficient heparinase activity, time of pretreatment, or only partial contribution of HSPG to peptide-mediated cholesterol reduction.
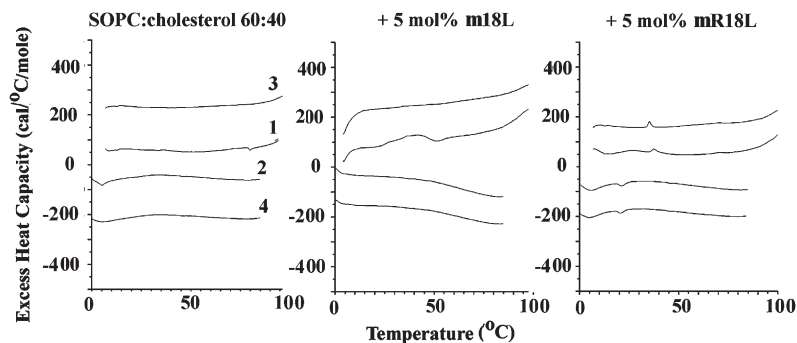
Bioavailability of peptide upon oral administration

Bioavailability of both ^{14}C-labeled m18L and mR18L were determined after both intravenous injection and gavage into apoE null mice. As shown in supplementary Fig. I, clearance of both peptides following intravenous injection was rapid and nearly identical for both peptides. In the gavage experiment, early time points were taken to determine time to maximum levels. Surprisingly, both peptides had a biphasic time course of entry, with a peak at 15 min and a second at 45 min (**Fig. 7A**). Although peptide mR18L had a somewhat lower first peak and higher second peak than m18L, the areas under the curve (AUC) were similar (Fig. 7B). Plasma taken 15 min postgavage was analyzed by reverse-phase HPLC for content of intact ^{14}C-labeled peptide and ^{14}C polar material (supplementary Fig. II). Of the radioactivity eluted from the column of plasma from mice gavaged with [^{14}C]mR18L, 43.3% eluted in the void volume as polar material, whereas 56.7% eluted in a position identical to the original peptide. In contrast, peptide m18L was essentially entirely intact, with no early-eluting polar peak (supplementary Fig. II). Similar analyses were not performed at later time points, as radioactivity in the plasma was insufficient for analysis. Plasma paraoxonase-1 activity and lipid hydroperoxide levels were measured following administration. No significant differences between the groups were found (data not shown).

Effect of oral administration of single-domain peptides on plasma cholesterol, lesion inhibition, and monocyte adhesion

Plasma cholesterol levels were determined in all the three groups at baseline (before the treatments were started), at midpoint of the experiment (three weeks), and at the end of the study period (six weeks). As shown in **Fig. 8A**, oral administration of the peptide mR18L, but not the

Fig. 4. Differential scanning calorimetry of SOPC:cholesterol (6:4) alone and with 5 mol% m18L or with 5 mol% mR18L. Scan rate 2K/min. Lipid concentration 2.5 mg/ml in 20 mM PIPES, 1 mM EDTA, and 150 mM NaCl with 0.002% NaN_3, pH 7.4. Sequential heating and cooling scans were done between 0 and 100°C. Numbers are the order in which the scans were carried out, with scans 1 and 3 being heating scans, each of which was followed by cooling scan 2 or 4. Scans are displaced along the Y axis for clarity of presentation. SOPC, stearoyloleoyl phosphatidylcholine.

Atheroprotective effects of an orally active L-peptide 3495

TABLE 1. Partition constants and free energy of binding of peptides m18L and mR18L to oxidized lipids

Lipid	m18L		mR18L		4F		2F	
	Kp	ΔG (kcal/mol)	Kp	ΔG (kcal/mol)	Kp	ΔG (kcal/mol)	Kp	ΔG (kcal/mol)
PGPC	3.4×10^6	-8.96	6.4×10^6	-9.34	1.6×10^7	-9.9	3.1×10^6	-8.9
Azelaoyl PAF	2.8×10^6	-8.85	3.9×10^6	-9.04	1.4×10^7	-9.8	2.7×10^6	-8.6
PVOPC	2.5×10^6	-8.78	4.3×10^6	-9.10	—	—	—	—

control peptide m18L, reduced plasma cholesterol levels significantly at both time points; i.e., at three weeks (9% reduction) and at six weeks (14% reduction) compared with baseline levels. Cholesterol profiles demonstrated that the reduction was entirely in the VLDL region (supplementary Fig. III). Plasma cholesterol values for control mice and m18L-treated mice were not different from their baseline levels. Thus, even though a small amount of the peptide enters plasma, it was effective in lowering cholesterol levels significantly.

Mice were euthanized at the end of six weeks for organ collection. The aortic sinus lesion area was measured. As shown in Fig. 8B, mice administered with peptide mR18L had significantly less atherosclerotic lesion area compared with the control and peptide m18L-treated mice. This finding is in accordance with the decrease in plasma cholesterol levels observed by this treatment.

As peptide mR18L was designed so that it possessed both cholesterol-lowering ability and anti-inflammatory properties, we analyzed the anti-inflammatory property of the peptide by determining its ability to inhibit the adhesion of monocytes to bovine aortic endothelial cells. We used lipopolysaccharide (LPS) treatment, which is known to enhance monocyte adhesion, as a positive control in this experiment. Adhesion of THP-1 monocytes to BAEC treated with LPS was 2-fold more than to cells that were not incubated with LPS and 1.3 times more than cells treated with plasma from apoE null mice (control). Plasma from control and m18L-treated groups enhanced monocyte adhesion to BAEC compared with cells that had not been treated. There was no significant difference between these samples. These results suggested the presence of

inflammatory molecules in the plasma from saline and m18L-administered mice that could induce adhesion molecules, such as VCAM-1, in BAEC, leading to increased adhesion of monocytes. In contrast, plasma from mR18L-administered mice showed no change in monocyte adhesion to BAEC compared with untreated control cells (**Fig. 9**), suggesting that mR18L has anti-inflammatory properties and
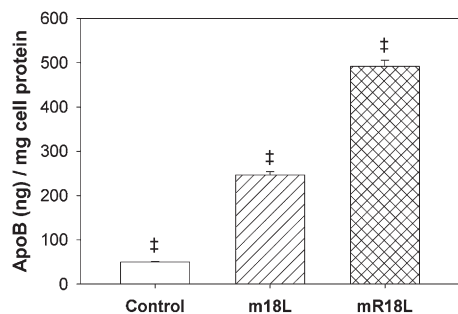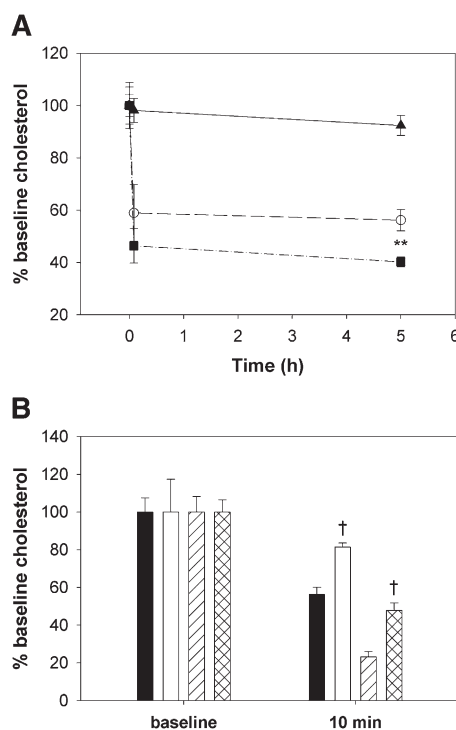

Fig. 6. Intravenous administration of m18L and mR18L decreases plasma cholesterol levels at least partially mediated by heparin sulfate proteoglycans. A: Vehicle (saline; ▲) and 75 μg of m18L (○) and mR18L (■) were injected into female apoE null mice intravenously. Blood was drawn at 0 min, 2 min, and 5 h after injection. Both peptides were effective in decreasing plasma cholesterol levels significantly at 2 min, and this continued up to 5 h. n = 3 in the saline group and 4 in each treatment group. Data are expressed as mean ± SEM. **$P < 0.025$; m18L versus mR18L. Both peptide groups were significantly different from the saline group at 5 min and 5 h ($P < 0.001$). B: The effect of proteoglycans on peptide-mediated cholesterol reduction was assessed by injected saline or heparinase (50 units/mouse; Sigma) intravenously 5 min before peptide injection. Data shown represent mean ± SEM (n = 6 in each group) for saline then m18L (black bars), heparinase then m18L (white bars), saline then mR18L (single hatched bars), and heparinase then mR18L (double-hatched bars). †$P < 0.001$, saline versus heparinase in each peptide group. All 10 min levels were significantly reduced compared with baseline ($P < 0.001$). Apo, apolipoprotein.
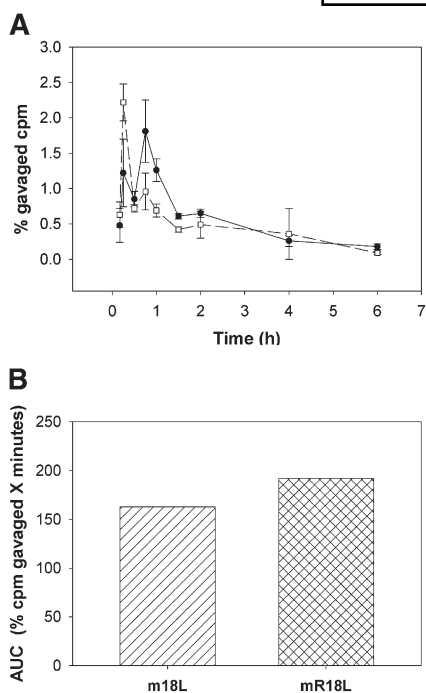

Fig. 5. Single-domain cationic peptides, mR18L and m18L, enhance LDL uptake by HepG2 cells. Uptake of ^{125}I-LDL was enhanced 5-fold by m18L (10 μg/ml; n = 6) and 10-fold by mR18L (10 μg/ml; n = 6). Data are expressed as mean ± SEM. ‡$P < 0.001$ denotes that all groups are significantly different from each other.

Fig. 7. Peptides m18L and mR18L are orally bioavailable. A: 112 μg of [^{14}C]m18L (□) and 100 μg of [^{14}C]mR18L (●) in saline were administered by gavage to female apoE null mice. Specific activity of m18L was 1.23×10^7, and mR18L, 4.83×10^6 cpm/mg peptide. Blood was drawn at various time points as indicated. Radioactivity in plasma at different time points (n = 3 per time point) was expressed as percent of gavaged cpm. Data are expressed as mean ± SEM. B: Area under the curve (AUC) was calculated for each peptide and is expressed as % injected cpm × minutes. Apo, apolipoprotein.

administration to apoE null mice ameliorates the inflammatory responses seen in control apoE null mice.

DISCUSSION

The arginine-containing peptide mR18L exhibits greater atheroprotective activity than its lysine-containing analog m18L (Figs. 8 and 9). Binding studies indicate that both peptides possess similar abilities to bind to human LDL and to the isolated lipoprotein fraction (d < 1.21 g/ml) from apoE null mouse plasma. Thus the difference in the biological activity does not appear to be due to binding to lipoproteins. Oral bioavailability studies also indicate that both peptides enter circulation at nearly equal levels (Fig.7A, B). Retro-orbital administration of 75 μg/mouse in female apoE null mice showed both the peptides reduced plasma cholesterol levels; the mR18L peptide was more effective than m18L (Fig. 6A), with at least some of this cholesterol reduction dependent on HSPG (Fig. 6B). These results are in agreement with the results obtained in vitro using hepatocytes (Fig. 5). Physical chemical properties studied by right-angle light scattering (Fig. 2) and DSC also indicate a greater interaction of mR18L with SOPC compared to m18L with SOPC (Figs. 3 and 4), as well as a greater ability to bind oxidized lipids compared to m18L (Table 1). The more potent sequestration of cholesterol in membranes with SOPC by mR18L is also consistent with
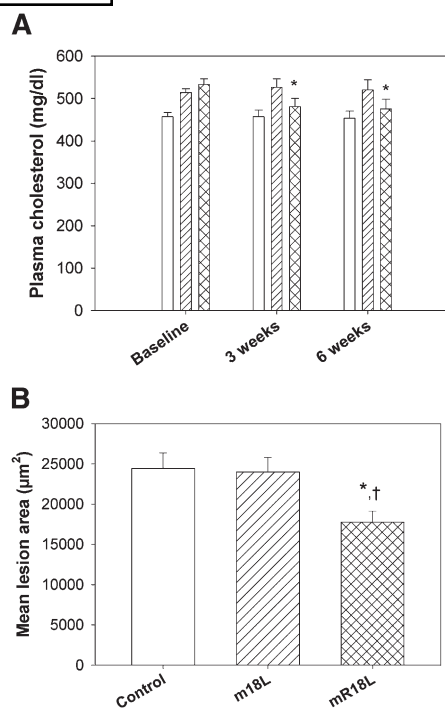

Fig. 8. Long-term oral administration of mR18L decreases plasma cholesterol levels and aortic sinus lesion formation. Four-week old female apoE null mice were fed with chow alone (open bar, n = 24), chow mixed with m18L (1 mg per 4 g chow, single hatched bar, n = 23) or mR18L (1 mg per 4 g chow, double hatched bar, n = 25) for six weeks. A: Plasma was analyzed for cholesterol levels at baseline, three weeks, and six weeks after beginning treatment. Peptide mR18L was effective in decreasing plasma cholesterol levels to a small, but significant extent (*$P < 0.05$) compared with baseline cholesterol in the same animals. Data are expressed as mean ± SEM. B: Oil Red O-stained area in aortic sinus was measured in all three groups at the end of treatment period. After six weeks of treatment, mice fed with peptide mR18L (double hatched bar) had significantly less atherosclerotic lesion area compared with control-fed (open bar, $^†P < 0.01$) and with peptide m18L-fed (single hatched bar, *$P < 0.05$) mice. Data are expressed as mean ± SEM. Apo, apolipoprotein.

this peptide having a greater affinity for the SOPC component of the mixture and, therefore, being more effective in excluding cholesterol. This could potentially allow greater water penetration into the membrane (25), which has been postulated to correlate with anti-inflammatory properties (6). Several examples in the literature indicate that peptides with Arg penetrate membranes more deeply than the same peptides containing Lys, Arg being a crucial residue for the membrane insertion in cationic cell-penetrating peptides (CCP) (26). Recent evidence demonstrated that the guanidine groups of Arg residues in penetratin form hydrogen bonds with phosphate groups and that this interaction is important for the functioning of these peptides (27). This interaction had also been predicted by molecular dynamics studies (28). The ability of Arg-rich sequences to partition into a more hydrophobic phase also supports stronger membrane interactions of Arg compared with Lys (29).

Free-energy perturbation calculations to estimate the pK of an Arg side chain in a 7-dipalmitoyl phosphatidylcholine
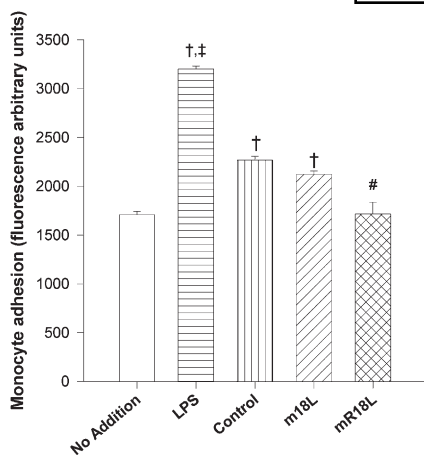
Fig. 9. Plasma of mR18L-treated apoE null mice inhibits monocyte adhesion to BAECs The effect of medium alone (n = 6), LPS (1 μg/ml; n = 6), plasma from control chow (n = 6, each pooled from two or three mice), m18L chow treated (n = 6, each pooled from two or three mice), or mR18L chow treated (n = 6, each pooled from two or three mice) apoE null mice on the adhesion of THP-1 monocytes to BAEC was measured as described in "Materials and Methods." Data are expressed as mean ± SEM. [†]$P < 0.01$ denotes a significant difference compared with "no addition" samples; [#]$P < 0.01$ denotes a significant difference compared with control chow plasma samples; [‡]$P < 0.007$ denotes a significant difference compared with control chow plasma samples. Apo, apolipoprotein; BAEC, bovine aortic endothelial cell.

(DPPC) bilayer support the idea that the lipid bilayer and water molecules can locally deform to stabilize the charged Arg side chain in a protein; as a result, Arg remains protonated in spite of the low dielectric nature of the bulk lipid membrane (30). In the context of these investigations, apoB-containing lipoproteins with mR18L would more strongly interact with hepatocytes for their clearance than those with m18L. A simple explanation is that the pKa for Arg is 12.5 compared with the 10.6 pKa of Lys. In addition, due to a nonshared positively charged guanidino group in Arg, the side chain of Arg is able of forming multiple H-bonds compared with the Lys side chain. This also potentially enhances affinity to oxidized lipids and negative surfaces, such as HSPG.

The main reasons for low oral bioavailability of peptide drugs would be expected to be presystemic enzymatic degradation and poor penetration of the intestinal mucosa. For example, bioavailability is very low for most oral protein delivery systems. This might only be acceptable for peptide drugs that are both cheap and safe. Recently Navab et al. showed that when L-4F was orally administered with niclosamide, it was able to inhibit atherosclerosis (31). Thus, an adjuvant such as niclosamide is needed for protecting the peptide from proteolytic degradation during oral delivery. However, when the peptides m18L and mR18L were administered by oral gavage, a small amount of intact peptide was found in the plasma. The peptide mR18L also reduced plasma cholesterol significantly compared with the Lys analog m18L. The peptide mR18L also exhibited potentially anti-inflammatory properties as determined by the BAEC assay (Fig. 9). In the current studies,

oral administration of mR18L, but not m18L, was effective in inhibiting atherosclerosis in apoE null mice. This is the first demonstration of an L-amino acid-containing peptide capable of inhibiting atherosclerosis when delivered orally in the absence of an adjuvant.▐▐▐

REFERENCES

1. Anantharamaiah, G. M., J. L. Jones, C. G. Brouillette, C. F. Schmidt, B. H. Chung, T. A. Hughes, A. S. Bhown, and J. P. Segrest. 1985. Studies of synthetic peptide analogs of the amphipathic helix: structure of complexes with dimyristoylphosphatidyl choline. *J. Biol. Chem.* **260:** 10248–10255.
2. Anantharamaiah, G. M. 1986. Synthetic peptide analogs of apolipoproteins. *Methods Enzymol.* **128:** 627–647.
3. Mendez, A. J., G. M. Anantharamaiah, J. P. Segrest, and J. F. Oram. 1994. Synthetic amphipathic helical peptides that mimic apolipoprotein A-I in clearing cellular cholesterol. *J. Clin. Invest.* **94:** 1698–1705.
4. Van Lenten, B. J., A. C. Wagner, G. M. Anantharamaiah, M. Navab, S. T. Reddy, G. M. Buga, and A. M. Fogelman. 2009. Apolipoprotein A-I mimetic peptides. *Curr. Atheroscler. Rep.* **11:** 52–57.
5. Navab, M., G. M. Anantharamaiah, S. Hama, D. W. Garber, M. Chaddha, G. Hough, R. Lallone, and A. M. Fogelman. 2002. Oral administration of an apo A-I mimetic peptide synthesized from D-amino acids dramatically reduces atherosclerosis in mice independent of plasma cholesterol. *Circulation.* **105:** 290–292.
6. Datta, G., R. F. Epand, R. M. Epand, M. Chaddha, M. A. Kirksey, D. W. Garber, S. Lund-Katz, M. C. Phillips, S. Hama, M. Navab, et al. 2004. Aromatic residue position on the nonpolar face of class A amphipathic helical peptides determines biological activity. *J. Biol. Chem.* **279:** 26509–26517.
7. Handattu, S. P., D. W. Garber, D. C. Horn, D. W. Hughes, B. Berno, A. D. Bain, V. K. Mishra, M. N. Palgunachari, G. Datta, G. M. Anantharamaiah, et al. 2007. ApoA-I mimetic peptides with differing ability to inhibit interactions with membrane bilayers. *J. Biol. Chem.* **282:** 1980–1988.
8. Anantharamaiah, G. M., V. K. Mishra, D. W. Garber, G. Datta, S. P. Handattu, M. N. Palgunachari, M. Chaddha, M. Navab, S. T. Reddy, J. P. Segrest, et al. 2007. Structural requirements for anti-oxidative and anti-inflammatory properties of apo A-I mimetic peptides. *J. Lipid Res.* **48:** 1915–1923.
9. Epand, R. F., V. K. Mishra, M. N. Palgunachari, G. M. Anantharamaiah, and R. M. Epand. 2009. Anti-inflammatory peptides grab on to the whiskers of atherogenic oxidized lipids. *Biochim. Biophys. Acta.* **1788:** 1967–1975.
10. Shimano, H., N. Yamada, M. Katsuki, K. Yamamoto, T. Gotoda, K. Harada, M. Shimada, and Y. Yazaki. 1992. Plasma lipoprotein metabolism in transgenic mice overexpressing apolipoprotein E. Accelerated clearance of lipoproteins containing apoE. *J. Clin. Invest.* **90:** 2084–2091.
11. Mahley, R. W., K. H. Weisgraber, M. M. Hussein, B. Greenman, M. Fishe, T. Vogel, and M. Gorecki. 1989. Intravenous infusion of apolipoprotein E accelerates clearance of plasma lipoprotein in rabbits. *J. Clin. Invest.* **83:** 2125–2130.
12. Zhang, S. H., R. L. Reddick, J. A. Piedrahita, and N. Maeda. 1992. Spontaneous hypercholesterolemia and arterial lesions in mice lacking apolipoprotein E. *Science.* **258:** 468–471.
13. Datta, G., M. Chaddha, D. W. Garber, B. H. Chung, E. M. Tytler, N. Dashti, W. A. Bradley, S. H. Gianturco, and G. M. Anantharamaiah. 2000. The receptor binding domain of apolipoprotein E linked to a model class A amphipathic helix enhances internalization and degradation of LDL by fibroblasts. *Biochemistry.* **39:** 213–220.
14. Gupta, H., C. R. White, S. Handattu, D. W. Garber, G. Datta, M. Chaddha, L. Dai, S. H. Gianturco, W. A. Bradley, and G. M. Anantharamaiah. 2005. An apoE mimetic peptide dramatically lowers plasma cholesterol and restores endothelial function in Watanabe Heritable Hyperlipidemic rabbits. *Circulation.* **111:** 3112–3118.
15. Garber, D. W., S. Handattu, I. Aslan, G. Datta, M. Chaddha, and G. M. Anantharamaiah. 2003. Effect of an arginine-rich amphipathic helical peptide on plasma cholesterol in dyslipidemic mice. *Atherosclerosis.* **168:** 229–237.
16. Tytler, E. M., J. P. Segrest, R. M. Epand, S. Q. Nie, R. F. Epand, V. K. Mishra, Y. V. Venkatachalapathi, and G. M. Anantharamaiah. 1993. Reciprocal effects of apolipoprotein and lytic peptide analogs

on membranes. Cross-sectional molecular shapes of amphipathic alpha-helixes control membrane stability. *J. Biol. Chem.* **268:** 22112–22118.

17. Van Lenten, B. J., A. C. Wagner, C-L. Jung, P. Ruchala, A. J. Waring, R. I. Lehrer, A. D. Watson, S. Hama, M. Navab, G. M. Anantharamaiah, et al. 2008. Anti-inflammatory apoA-I-mimetic peptides bind oxidized lipids with much higher affinity than human apoA-I. *J. Lipid Res.* **49:** 2302–2311.

18. Mishra, V. K., M. N. Palgunachari, J. P. Segrest, and G. M. Anantharamaiah. 1994. Interactions of synthetic peptide analogs of the class A amphipathic helix with lipids. Evidence for the snorkel hypothesis. *J. Biol. Chem.* **269:** 7185–7191.

19. Privalov, G., V. Kavina, E. Freire, and P. L. Privalov. 1995. Precise scanning calorimeter for studying thermal properties of biological macromolecules in dilute solution. *Anal. Biochem.* **232:** 79–85.

20. Goldstein, J. L., S. K. Basu, and M. S. Brown. 1983. Receptor-mediated uptake of low density lipoproteins in cultured cells. *Methods Enzymol.* **98:** 241–260.

21. Garber, D. W., G. Datta, M. Chaddha, M. N. Palgunachari, S. Y. Hama, M. Navab, A. M. Fogelman, J. P. Segrest, and G. M. Anantharamaiah. 2001. A new synthetic class A amphipathic peptide analog protects mice from diet-induced atherosclerosis. *J. Lipid Res.* **42:** 545–552.

22. Garber, D. W., K. R. Kulkarni, and G. M. Anantharamaiah. 2000. A sensitive and convenient method for lipoprotein profile analysis of individual mouse plasma samples. *J. Lipid Res.* **41:** 1020–1026.

23. Datta, G., C. R. White, N. Dashti, M. Chaddha, M. N. Palgunachari, H. Gupta, S. P. Handattu, and G. M. Anantharamaiah. 2010. Anti-inflammatory and recycling properties of an apolipoprotein mimetic peptide, Ac-hE18A-NH₂. *Atherosclerosis.* **208:** 134–141.

24. Epand, R. M. 2007. Detecting the presence of membrane domains using DSC. *Biophys. Chem.* **126:** 197–200.

25. Epand, R. M., R. F. Epand, B. G. Sayer, G. Melacini, M. N. Palgulachari, J. P. Segrest, and G. M. Anantharamaiah. 2004. An apolipoprotein AI mimetic peptide: membrane interactions and the role of cholesterol. *Biochemistry.* **43:** 5073–5083.

26. Esbjorner, E. K., P. Lincoln, and B. Norden. 2007. Counterion-mediated membrane penetration: cationic cell-penetrating peptides overcome Born energy barrier by ion-pairing with phospholipids. *Biochim. Biophys. Acta.* **1768:** 1550–1558.

27. Su, Y., T. Doherty, A. J. Waring, P. Ruchala, and M. Hong. 2009. Roles of arginine and lysine residues in the translocation of a cell-penetrating peptide from (13)C, (31)P, and (19)F solid-state NMR. *Biochemistry.* **48:** 4587–4595.

28. Herce, H. D., and A. E. Garcia. 2007. Molecular dynamics simulations suggest a mechanism for translocation of the HIV-1 TAT peptide across lipid membranes. *Proc. Natl. Acad. Sci. USA.* **104:** 20805–20810.

29. Rothbard, J. B., T. C. Jessop, R. S. Lewis, B. A. Murray, and P. A. Wender. 2004. Role of membrane potential and hydrogen bonding in the mechanism of translocation of guanidinium-rich peptides into cells. *J. Am. Chem. Soc.* **126:** 9506–9507.

30. Yoo, J., and Q. Cui. 2008. Does arginine remain protonated in the lipid membrane? Insights from microscopic pKa calculations. *Biophys. J.* **94:** L61–L63.

31. Navab, M., P. Ruchala, A. J. Waring, R. I. Lehrer, S. Hama, G. Hough, M. N. Palgunachari, G. M. Anantharamaiah, and A. M. Fogelman. 2009. A novel method for oral delivery of apolipoprotein mimetic peptides synthesized from all L-amino acids. *J. Lipid Res.* **50:** 1538–1547.